Interface focus

J. R. Soc. Interface (2008) **5**, S161–S168
doi:10.1098/rsif.2008.0249.focus
Published online 29 July 2008

Spatially selective sampling of single cells using optically trapped fusogenic emulsion droplets: a new single-cell proteomic tool

Peter M. P. Lanigan[1], Karen Chan[1], Tanya Ninkovic[1], Richard H. Templer[1,2], P. M. W. French[1,3], A. J. de Mello[1,2], K. R. Willison[2,4], P. J. Parker[1,5], M. A. A. Neil[1,3,*], Oscar Ces[1,2,*] and D. R. Klug[1,2]

[1]*The Single Cell Proteomics Group, Chemical Biology Centre (CBC), [2]Department of Chemistry, and [3]Department of Physics, Imperial College London, Exhibition Road, London SW7 2AZ, UK*
[4]*The Institute of Cancer Research, Chester Beatty Laboratories, 237 Fulham Road, London SW3 6JB, UK*
[5]*Cancer Research UK, Lincoln's Inn Fields, London WC2A 3PX, UK*

We present a platform for the spatially selective sampling of the plasma membrane of single cells. Optically trapped lipid-coated oil droplets (*smart droplet microtools*, SDMs), typically 0.5–5 μm in size, composed of a hexadecane hydrocarbon core and fusogenic lipid outer coating (mixture of 1,2-dioleoyl-phosphatidylethanolamine and 1,2-dioleoyl-*sn*-glycero-3-phosphatidylcholine) were brought into controlled contact with target colon cancer cells leading to the formation of connecting membrane tethers. Material transfer from the cell to the SDM across the membrane tether was monitored by tracking membrane-localized enhanced green fluorescent protein.

Keywords: single-cell proteomics; optical trapping; plasma membrane; protein levels; membrane tether; emulsion

1. INTRODUCTION

Evidence for cellular heterogeneity (Ferrell & Machleder 1998; Huang *et al.* 2000; Teruel & Meyer 2002; Marcus *et al.* 2006) is now widespread, with the variation in gene expression and cell-to-cell variability in normal tissue caused by many factors. These can include different cellular environments or phases in the cell cycle or just the fluctuations caused by the statistics of small numbers. Given the temporal variations within a cell, some proteins might be extremely plentiful at one time and scarcely abundant at another. They can also demonstrate properties that change over time through a range of post-translational modifications. As it becomes increasingly clear that cells within a given population are heterogeneous in important ways, the use of single-cell methods in order to understand cell responses to therapeutic interventions and disease states is becoming increasingly important (Roman *et al.* 2007; Sims & Allbritton 2007).

Recent technological developments are beginning to open up the possibility of measuring protein expression levels in single cells (Zhang & Jin 2006; Huang *et al.* 2007) but most standard approaches invariably involve fluorescence-based platforms. While labelling two or even three proteins together in this way is possible, the parallel analysis and quantification of larger numbers of species is currently beyond the tools and techniques available. We present a novel platform technology based on optically trapped smart droplet microtools (SDMs), which is suited to the study of membrane proteins from a single cell and could ameliorate this problem by performing spatially specific upstream separation of the plasma membrane.

There are also cases where the number of cells available is highly limited due to either their scarcity or the practical and ethical difficulties in obtaining them in large numbers. Under these circumstances, the development of tools aimed at facilitating the analysis of single or small numbers of cells is also beneficial.

1.1. A new approach to the isolation of proteins

The conventional method for isolating proteins is to lyse the total content of an ensemble of cells, and then to use a series of increasingly specific purification steps to isolate the required protein species. Examples of more targeted approaches to lysis include *in vivo* surface labelling followed by lysis and affinity capture

*Authors and addresses for correspondence: M. A. A. Neil, Department of Physics, Imperial College London, Exhibition Road, London SW7 2AZ, UK (mark.neil@imperial.ac.uk); O. Ces, Department of Chemistry, Imperial College London, Exhibition Road, London SW7 2AZ, UK (o.ces@imperial.ac.uk).

One contribution of 7 to a Theme Supplement 'Single-cell analysis'.

Received 9 June 2008
Accepted 7 July 2008

(Peirce *et al.* 2004), with membrane proteins usually somewhat harder to handle than water-soluble proteins. The usual strategy is to solubilize as much of the membrane as possible and then separate it. However, the majority of proteins extracted by this process and subsequently identified by mass spectrometry, for example, are not membrane proteins, as these typically constitute only 10–20 per cent of the proteins recovered (Han *et al.* 2001; Washburn *et al.* 2001; Blonder *et al.* 2002).

Microfluidic systems are being developed with a view to effecting single-cell analysis (Schilling *et al.* 2002; Quinto-Su *et al.* 2008), with established systems including modules for controlling the position of a target cell, lysis of the entire cell, collection and separation of the lysed components and analysis of the intracellular components. Reported on-chip approaches for complete single-cell lysis include microfluidic systems based on the application of laser pulses (Rau *et al.* 2006), electrical fields (Zimmerberg & Kozlov 2006), mechanical shear forces (Di Carlo *et al.* 2003) and chemical treatment (Ocvirk *et al.* 2004). While these systems offer increasingly sophisticated levels of control with respect to full cell disruption, most require downstream separation steps in order to achieve subcellular specificity. Currently, spatially specific membrane extraction can be performed using capillary-based methods (Jonsson & Mathiasson 2000) and patch-clamp techniques. In patch-clamping experiments, the micropipette tips used to probe the cell surface can be heated in a microforge to produce a smooth surface that results in the formation of a gigaseal with the cell membrane. After the gigaseal is formed, if the electrode is quickly withdrawn from the cell (inside-out patch-clamp configuration; Sakmann & Neher 1984), a patch of membrane can be ripped off the cell. Bradke & Dotti (1999) and, more recently, Takayama *et al.* (2003) have shown that it is now possible to deliver reagents to and from cells with subcellular specificity using a combination of micromanipulators and laminar streams in microfluidic devices (PARTCELL) that could be adapted to drive localized membrane disruption.

We present an approach in which we deliberately avoid solubilizing the whole membrane and, instead, perform stepwise spatially selective sampling of the plasma membrane of single cells under controlled conditions. This approach has the potential to reduce the problem caused by high-abundance proteins (including cytosolic systems) masking low-abundance ones and achieve spatially selective sampling of a cell, thereby simplifying the problem of separation downstream by tackling it upstream of any analysis modules.

1.2. Nanodigestion

It has previously been demonstrated that the plasma membrane of a cell can be manipulated by physical contact with modules such as polystyrene beads (Raucher & Sheetz 1999; Li *et al.* 2002). In these studies, plasma membrane-attached polystyrene beads were pulled away from a cell using optical tweezers, resulting in the formation of a membrane tube, and used to characterize the biomechanical properties of the plasma membrane. Such protocols are inherently limited by the physical characteristics of the bead that restrict their use as modules for either the uptake or delivery of material to a cell.

We have overcome these issues by using fluid-based SDMs as the triggers for membrane tether formation and reservoirs for the storage of extracted plasma membrane material during a process termed *nanodigestion*. Cell–SDM interactions are controlled using optical traps and monitored via a combination of bright field and fluorescence imaging. The SDM itself can be visualized as consisting of defined interior and exterior regimes (figure 1*c*), wherein the interior consists of hydrophobic hexadecane (Ward *et al.* 2006) whose refractive index differs sufficiently from that of water to allow it to be manipulated using optical tweezers. Other oils can be used, but our measurements (data not shown) demonstrated that SDM stability was optimum for hexadecane/water assemblies. The coating of the SDMs comprises a mixture of amphiphilic molecules, 1,2-dioleoyl-phosphatidylethanolamine (DOPE; figure 1*b*) and 1,2-dioleoyl-*sn*-glycero-3-phosphocholine (DOPC; figure 1*c*), which form inverse hexagonal (figure 1*d*; Seddon 1990) and fluid lamellar phases (figure 1*e*), respectively, under excess water conditions.

2. MATERIAL AND METHODS

2.1. Laser trapping and fluorescence imaging

All trapping experiments were conducted on a Nikon TE2000-E automated microscope, with custom-built laser trapping optics suspended from the external rear port for two-beam optical manipulation (figure 2). The cage plate-based optical system (a combination of Linos Photonics, Qioptiq and Thorlabs Ltd parts), which extended out from the modified supporting block (SB) of the microscope objective turret, allowed for compact and safe containment of the beam without the requirement for any further optics on the bench. Furthermore, the compact fibre-coupled laser source with diffraction-limited beam quality (IPG Photonics, YLM-5, 5 W, 1070 nm, linearly polarized) was directly fed into the trapping optics by a set of custom-made cage plates (I1).

To facilitate the manipulation of two traps, an optical arrangement was constructed using a polarizing beam splitter (B1), two quarter-wave plates ($\lambda/4$) and two steering mirrors (M1 and M2). The linearly polarized input laser at an angle of 45° was then split and recombined into two independent beams of opposite polarization, which were manoeuvred by the mirrors independently.

Plane mirror mounts placed at each arm of the interferometer were modified in-house for the fitting of linear actuators (A1–4; NSA-12, Newport, 11 mm range, 0.1 µm resolution), which allowed for precision steering of the optical traps in the x–y plane. The actuators were connected up to an eight-axis switch box and hand-held controller (NSC-SB and NSC-200, respectively, Newport) and computer interfaced via an RS-485 to RS-232 converter (NSC-485-232-I, Newport) as part of the NewStep Expandable Motion Controller

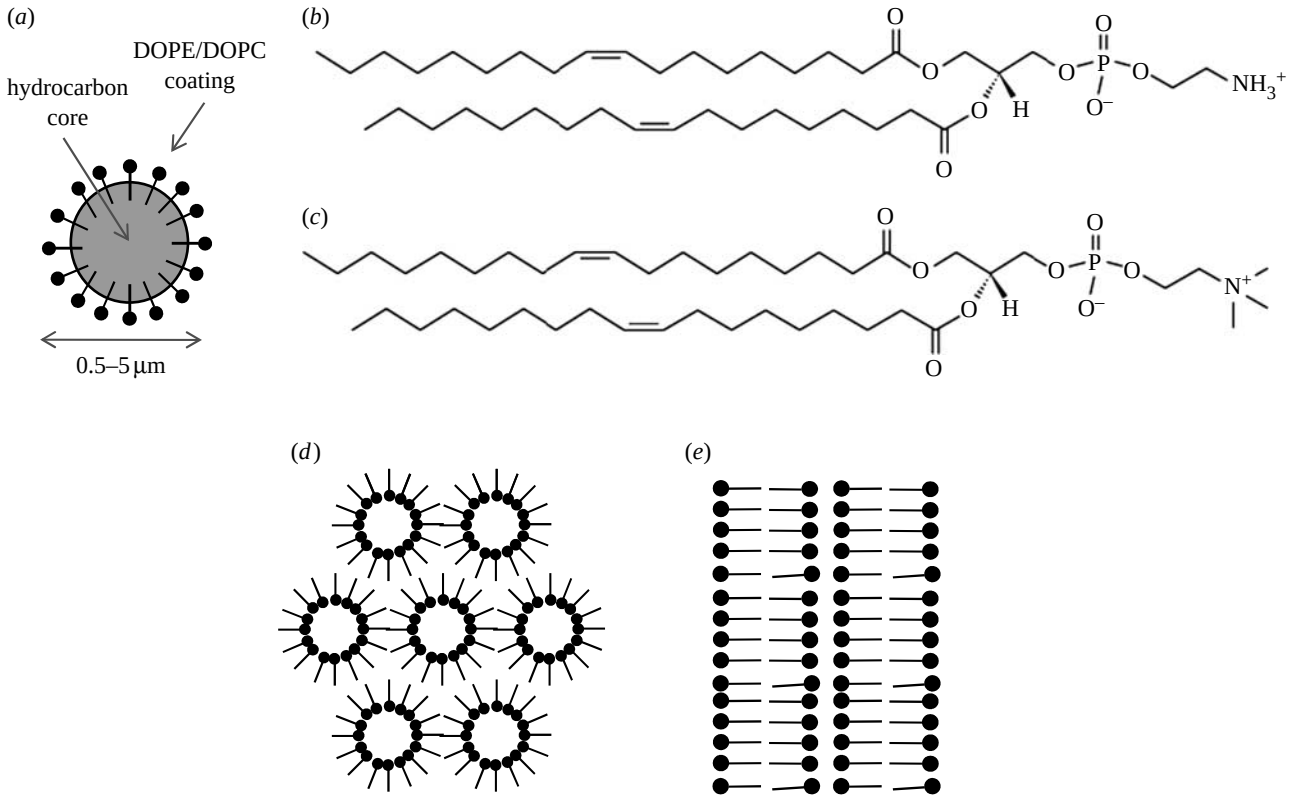

Figure 1. (*a*) Schematic of an SDM and structures of (*b*) 1,2-dioleoy-phosphatidylethanolamine, (*c*) 1,2-dioleoyl-phosphatidylcholine, (*d*) the inverse hexagonal phase and (*e*) the lamellar phase.

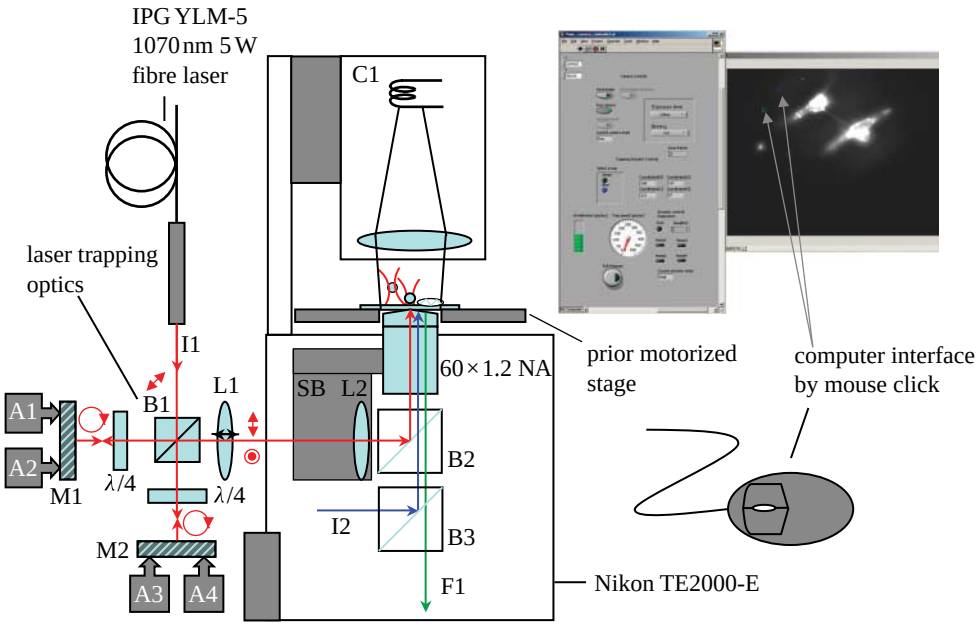

Figure 2. A schematic of a trapping microscope used in experiments with traps controlled by a custom-written LabView point–click interface. I1, trapping laser input; B1, polarizing beam splitter; M1–2, IR 1064 nm dielectric mirrors; $\lambda/4$, quarter-wave plates; A1–4, computer-controlled stepper motors; L1, focal length = 100 mm planovex IR AR-coated refocusing lens; L2, focal length = 100 mm planovex IR AR-coated lens; SB, SB of the microscope turret; B2, IR trapping dichroic; B3, FITC dichroic; I2, mercury lamp excitation input; Fl, fluorescence output to camera/eyepiece; C1, bright field condenser and lamp housing; NA, numerical aperture.

System (Newport). These mirrors were then imaged using a 1× telescope (L1 and L2) onto the pupil plane of the microscope objective (60× 1.2 numerical aperture, water immersion, Nikon) to minimize the loss of power of the trapping beams when steering the traps in the image plane. No beam expansion was required as the output diameter of the fibre laser was 8 mm, which was sufficiently large to fill the objective pupil. Refocusing of the traps was achieved by sliding the lens (L1) in and out.

The trapping dichroic (B2; Z900DCSP, Chroma) was located below the microscope objective and held into position by the SB of the microscope objective turret. Below the trapping dichroic was situated a filter cube carousel incorporating a FITC cube (B3) used for mercury lamp excitation (I2) and epifluorescence imaging (Fl) of enhanced green fluorescent protein (EGFP)-labelled cells.

Both bright field images obtained by the transillumination system (C1) and fluorescence images were captured by a cooled digital camera (ORCA-ER; Hamamatsu) situated on the left side port (100% transmission side) of the microscope. For fast screening of cells and manoeuvring of SDMs in the sample plane, a motorized x–y stage was used (Proscan; Prior).

The actuators were operated via an in-house LabView program (LabView v. 8.1; National Instruments) and allowed the traps to be positioned in the field of view of a 512×512 pixel image by a mouse click, where the location of the trap was indicated by an overlaid coloured square. In this case, the interface was such that the trap would move sequentially along the x-axis of the image followed by a movement along the y-axis. The speed and acceleration of the traps could be controlled by dials and sliders on the program's front panel. The LabView program also featured camera control including exposure time, binning and digital zoom and saved images in either 8 or 16 bit.tif format.

2.2. Cell culture protocols

Prior to cell splitting, 12 coverglass slides (22×22 mm, no. 1.5, VWR) were thoroughly cleaned in a disposable sterile large round Petri dish in 70 per cent ethanol/1 per cent HCl, dried in the biosafety cabinet and coated with poly-L-lysin according to the manufacturer's protocol.

Adherent BE human colon carcinoma cells expressing EGFP-Tk (EGFP-labelled CAAX motive of K-Ras) at the plasma membrane (Apolloni *et al.* 2000) were a kind gift from Dr Hugh Paterson at The Institute of Cancer Research, London. The cells were grown at 37°C and 5 per cent CO_2 in 25 ml filter-capped flasks containing phenol-free medium (high glucose DMEM; GibCo) with 10 per cent foetal calf serum, 100 µl ml^{-1} penicillin and 100 µg ml^{-1} streptomycin. These were then split when reaching 80 per cent confluency in a culture hood by the removal of culture medium, washing with sterile phosphate buffered saline (PBS, pH 7.4; GibCo) and incubation with 2 ml of trypsin solution (Sigma) containing trypsin 5 g ml^{-1} and EDTA 2 g ml^{-1} diluted to 10 per cent in PBS for 2–3 min. Once cells were detached, 5 ml of culture medium was added to the flask and the cells were gently resuspended by pipetting up and down for 30 s.

Then, 0.5 ml of cells was carefully pipetted onto the centre of each of the coverglass slides before being placed in the wells of 2×6 well plates. The well plate was then transferred into the incubator for 15 min while the cells attached to the glass. The plates were then removed from the incubator and a further 2–3 ml of culture medium was then added gently to each side of the wells before being returned to the incubator for 24 hours in order to allow the cells to polarize.

2.3. Fusogenic emulsion stock production

Anhydrous frozen lipid stocks of DOPE and DOPC were mixed in the required molar ratio of 3 : 1 and 5 mg of this mixture was added to a clean glass vial containing 2 ml of hexadecane (density = 0.773 g cm^{-3}) and 5 ml of single distilled water.

The mixture was then vortexed for a few seconds to form a stable cloudy oil-in-water emulsion that was observed not to ripen over the course of at least a week. Oils with shorter or longer chains separated into water and oil phases in a few minutes.

2.4. Experimental procedure (SDM–cell interactions)

Coverglass slides prepared as described in §2.2 were transferred onto the microscope slide holder. The emulsion stock solution (§2.3) was then diluted by a factor of 1 : 100 in clean PBS, shaken vigorously by hand and vortexed for 30 s, in order to redisperse the system. Then, 5–10 µl of this solution was pipetted onto the coverglass to which the polarized cells were adhered using a Gilson pipette. To prevent the drying out of the cells, they were kept covered with 200 µl of growth medium.

The LabView program was then initiated and a manual search using the motorized stage was used to locate and optically trap appropriate SDMs (sized between 1 and 5 µm). Once an SDM was trapped (laser powers used were typically approximately 200 mW at the pupil plane of the objective, typically approximately 40–60% transmission to the sample plane at 1070 nm; Neuman *et al.* 1999), the motorized stage was used again to locate a suitably polarized and EGFP-expressing cell. The SDM was eased up to the cell membrane so that contact was made and left to incubate next to the cell for 10–15 s. It was found that shorter incubation times were not sufficient to promote SDM–cell fusion and that, at greater incubation times, the SDM could not be detached from the cell surface.

After 15 s of contact, the SDM was moved away from the cell at a rate of approximately 0.5 µm s^{-1}. As a control, the laser beam was fixed on the cell membrane for a period of 10–15 s and moved away at the same rate, where upon no tether was observed.

2.5. Study of droplet fusogenicity

In order to assess the fusogenicity of DOPC/DOPE/hexadecane SDMs, the DOPC/DOPE/excess water phase diagram was constructed between 0 mol% DOPC/100 mol% DOPE/excess water and 100 mol% DOPC/0 mol% DOPE/excess water in steps of 10 mol%.

DOPC and DOPE were obtained from Avanti Polar Lipids, Inc. (Alabaster, AL, USA) with their purity stated to be greater than 97 per cent pure. Both were stored at −20°C before being lyophilized under vacuum for 48 hours and weighed as a function of time to ensure that any excess water was removed. To make a given DOPC/DOPE sample, each lipid was freeze-dried, weighed and then dissolved in chloroform forming

clear stock solutions of known concentration. In order to generate homogeneous binary mixtures, these solutions were then pipetted together in a glass vial to give the desired molar ratio and mixed thoroughly by vortexing. The chloroform was then evaporated off under nitrogen gas and the sample put back onto the lyophilizer overnight. Lipid mixtures were then transferred to a 1.5 mm glass capillary and water added (75 wt% water). The capillary was then spun down in a centrifuge, sealed and homogenized by means of four freeze–thaw mixing cycles. The sealed capillary was then placed in the sample holder of the X-ray beamline and weighed before and after to ensure no loss of water.

The phase behaviour of this binary system was measured using small-angle X-ray scattering (SAXS). SAXS measurements were conducted by means of an in-house custom-built X-ray beamline. A Bede Microsource (Durham, UK) generator was used to produce the focused Cu K_α (1.542 Å) radiation after filtering out the K_β (1.3922 Å) with a nickel filter coupled with low-divergence (2 mrad) monolithic polycapillary optics (X-ray Optical Systems, Inc., XOS-Albany, New York, USA). A Gemstar HS-intensified CCD (Photonic Science Ltd, Battle, UK) was used to record the two-dimensional diffraction patterns. The detector–PC interface was established using a digital LVDS (RS-644) Picasso PCI-LS framegrabber card from ARVOO Imaging products (The Netherlands). Sample capillaries (1.5 mm in diameter) were located in a copper sample holder with a Peltier (Melcor, NJ, USA)-driven temperature controller supported by a circulating water heat exchanger. This assembly was able to control the sample temperature to an accuracy of ± 0.1°C. Typical exposure times were 30 s.

The diffraction patterns were analysed with the AXcess software package developed by Andrew Heron at Imperial College London. X-ray measurements were calibrated with silver behenate ($d_{001} = 58.38$ Å).

3. RESULTS AND DISCUSSION

The role of compartmentalization played by biological membranes requires that cellular systems maintain a balance of lipids *in vivo* such that these complex mixtures form flat bilayer arrangements despite the fact that the same is not necessarily true of the individual lipids in isolation. When mixed with water for instance, type 0 lipids (Seddon 1990) such as phosphatidylcholine lipids (e.g. 1,2-dioleoyl-phosphatidylcholine) tend to form flat bilayer arrangements that include the fluid lamellar mesophase (figure 1*e*). This is in contrast to the type II phosphatidylethanolamines (e.g. DOPE) that tend to form curved interfaces where the plane of the headgroups curves towards the water leading to the formation of two-dimensional structures such as the inverse hexagonal phase (figure 1*d*). Type II lipids are implicated in a wide variety of dynamic fusion processes *in vivo* where topological rearrangement of a membrane is required. The propensity of type II lipids to form curved mesophases is reflected in part by the non-deformed unstressed curvature of the membrane that is commonly referred to as the spontaneous curvature of the membrane bilayer, J_S^B (Zimmerberg & Kozlov 2006). The effective spontaneous curvature of DOPE has been reported as $-(1/3)$ nm^{-1} (Leikin *et al.* 1996) in contrast to that of DOPC that lies between $-(1/20)$ nm^{-1} and $-(1/8.7)$ nm^{-1} (Chen & Rand 1997; Szule *et al.* 2002). By coating SDMs with binary DOPC/DOPE coatings, it should therefore be possible to fine-tune the propensity of these assemblies to undergo fusion with a target membrane.

In order to assess the fusogenicity of the SDMs coated with DOPC/DOPE mixtures, the phase behaviour of the DOPC/DOPE excess water system was measured (data not shown). Only compositions observed to form an inverse hexagonal phase at room temperature or above were subsequently employed as coatings for the SDMs, as these compositions were expected to promote fusion to a greater extent than those shown to form the lamellar phase.

In both the cases of the inverse hexagonal and fluid lamellar phases, a minimum of three peaks was used to assign the nature of the mesophase. The H_{II} phase gave rise to Bragg peaks in the ratio of $1 : \sqrt{3} : 2 : \sqrt{7}$ and the lamellar phase in the ratio of 1 : 2 : 3. Samples between 100 mol% DOPC/excess water and 55 mol% DOPE/45 mol% DOPC/excess water exclusively formed the fluid lamellar phase between 0 and 75°C. At 60 mol% DOPE/40 mol% DOPC/excess water, a transition from the fluid lamellar phase was observed at 75°C with the transition temperature dropping sharply to 45°C at 65 mol% DOPE/35 mol% DOPC/excess water and 25°C at 70 mol% DOPE/30 mol% DOPC/excess water. For both the 65 mol% DOPE/35 mol% DOPC/excess water and 70 mol% DOPE/30 mol% DOPC/excess water samples, the inverse hexagonal phase was found to coexist with the fluid lamellar phase up to 60 and 55°C, respectively. At 85 mol% DOPE/15 mol% DOPC/excess water, the inverse hexagonal phase was observed to coexist with the fluid lamellar phase between 5 and 25°C, and samples containing greater than 85 mol% DOPE were observed to form only the inverse hexagonal phase over the range of temperatures examined. In the light of these results, SDMs with coatings containing a minimum of 75 mol% DOPE were considered.

Using the protocols described in §2.4, BE human carcinoma cell–SDM interactions were monitored using a combination of bright field and fluorescence microscopy.

Figure 3 depicts one such experiment where trypsinized BE human carcinoma cells expressing membrane-localized EGFP were pipetted onto a clean coverglass followed by the addition of 10 µl of diluted SDM solution. The tether formation was observed following a 10 s incubation time with the BE cell plasma membrane, as shown in figure 3*b*,*c*. By trapping the SDM rather than the cell, we aimed to minimize the effects of sample heating that have been measured to be 2–3°C after 10 s for directly trapped Chinese hampster ovary cells (Liu *et al.* 1995). As can be seen from figure 3, the membrane tether was extended at a rate of 0.5 µm s^{-1} with a laser power of 150 mW. Below 100 mW, extraction rates exceeding 0.5 µm s^{-1} often resulted in detachment between the SDM and the tether. Typical lengths of the tether observed were between 10 and 30 µm (greater than the cell diameter), consistent with previous

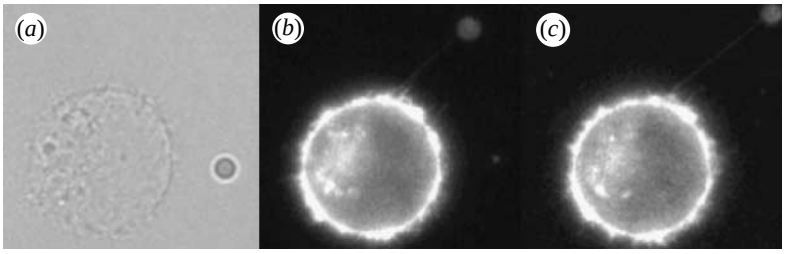

Figure 3. (*a*) A bright field image showing an SDM prior to contact with a BE cell. (*b*,*c*) Fluorescence images of an SDM pulling the tether from a BE cell at a rate of 0.5 μm s^{-1}. Scale bar, SDM size = 2.9 μm.

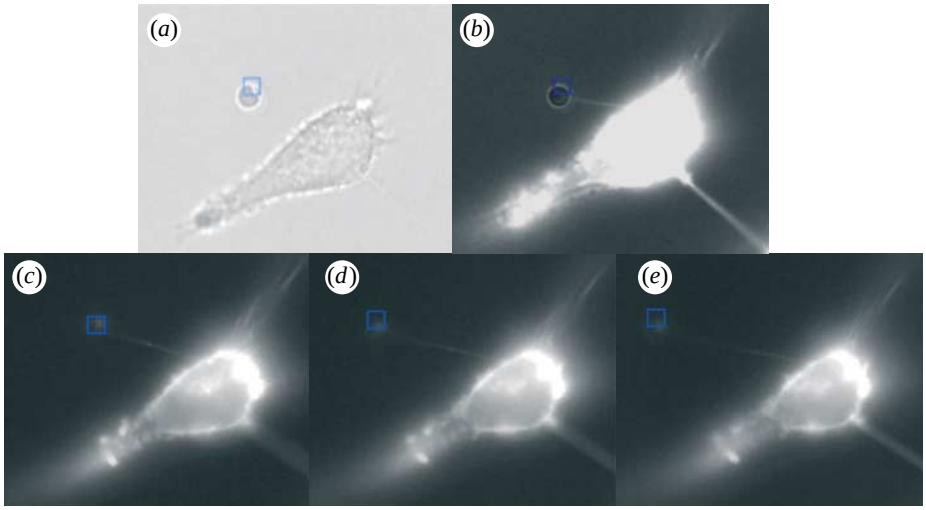

Figure 4. (*a*) A bright field image of an SDM (blue square) after contact with a polarized untrypsinized human BE cell, (*b*) a simultaneously acquired bright and fluorescence image and (*c*–*e*) a series of fluorescence images showing the pulling of the tether by an SDM at a rate of 0.5 μm s^{-1}. The blue square indicates approximate trap location due to a small amount of hysteresis in actuator movement. Scale bar, size of the square = 3 × 3 μm.

observations reported for tethers pulled from cochlear outer hair cells (Li *et al.* 2002), neuronal growth cones (Hochmuth *et al.* 1996) and red blood cells (Waugh & Bauserman 1995; Hwang & Waugh 1997) using latex beads. The efficiency of SDM–plasma membrane tether formation was over 80 per cent, with failure mainly due to incubation times exceeding 20 s whereupon the SDMs were observed to irreversibly fuse with the target cell irrespective of trapping power.

Although an 80 per cent success rate was observed for membrane tether formation with trypsinized cells, they provide a relatively facile target for tether formation, as the process of trypsinization leads to the digestion of the extracellular part of the transmembrane proteins that take part in intercellular adhesion or, indeed, adhesion to a container surface. There is therefore likely to be low resistance to fusion between the target cell and the SDM. In addition, if the SDMs are to be used as a proteomic tool for sampling the plasma membrane, it is beneficial to restrict any such modifications to the cell surface, particularly with a view to conducting time-dependent studies. To further explore the potential of SDMs as a tool for sampling the plasma membrane of single-cell systems, we therefore examined their mode of interaction with adherent non-trypsinized polarized BE cells grown on coverglasses (figure 4*a*–*e*). Again, a success rate of over 80 per cent was observed for tether formation using identical experimental protocols.

A key observation in both the trypsinized and untrypsinized cell experiments is the uptake of EGFP-labelled CAAX motifs from the inner leaflet of the plasma membrane of the cell to not only the membrane tether but also the surface of the SDM itself. This observation confirms that the membrane tether does not consist solely of phospholipid material from the plasma membrane but also protein material contained therein. Whether the tether consists of a single bilayer junction or bilayer tube is unclear but the transfer of EGFP-labelled CAAX that is expressed on the inner leaflet on the membrane seems to indicate that the latter is more likely. In the future, it will also be important to ascertain whether uptake of protein material is dependent on the protein being integral or peripheral.

It should also be noted that the fluorescence signal from the SDM does not reach a threshold value during the 20 s contact time, meaning that longer incubation would result in even greater uptake of protein material. At present, the composition of the SDMs is such that these longer incubation times are not accessible due to permanent fusion of the two moieties but further exploration of the coating of the droplet should facilitate access to this regime.

4. CONCLUSIONS

We have demonstrated a novel technological platform for the process of *nanodigestion* that allows for selective sampling of the plasma membrane of target cells at the

single-cell level with both the spatial and temporal control, in effect, a molecular scale biopsy. The use of SDMs negates the destruction of the cell, allowing for repeated sampling of a given cell as a function of time and space. Coupled with suitable readout platforms such as fluorescence-based protein microarrays (Fournier *et al.* 2008) that offer the potential of low-copy-number protein identification, it may be possible to explore protein expression levels at the single level using SDMs as a sampling tool.

We thank the EPSRC for the award of grant EP/C54269X/1 and Platform grants GR/S77721 and EP/C541839/1. We would like to thank Dr Christopher Dunsby for establishing the optical platforms used during these experiments.

REFERENCES

Apolloni, A., Prior, I. A., Lindsay, M., Parton, R. G. & Hancock, J. F. 2000 H-ras but not K-ras traffics to the plasma membrane through the exocytic pathway. *Mol. Cell Biol.* **20**, 2475–2487. (doi:10.1128/MCB.20.7.2475-2487.2000)

Blonder, J., Goshe, M. B., Moore, R. J., Pasa-Tolic, L., Masselon, C. D., Lipton, M. S. & Smith, R. D. 2002 Enrichment of integral membrane proteins for proteomic analysis using liquid chromatography–tandem mass spectrometry. *J. Proteome Res.* **1**, 351–360. (doi:10.1021/pr0255248)

Bradke, F. & Dotti, C. G. 1999 The role of local actin instability in axon formation. *Science* **283**, 1931–1934. (doi:10.1126/science.283.5409.1931)

Chen, Z. & Rand, R. P. 1997 The influence of cholesterol on phospholipid membrane curvature and bending elasticity. *Biophys. J.* **73**, 267–276.

Di Carlo, D., Jeong, K. H. & Lee, L. P. 2003 Reagentless mechanical cell lysis by nanoscale barbs in microchannels for sample preparation. *Lab Chip* **3**, 287–291. (doi:10.1039/b305162e)

Ferrell, J. E. & Machleder, E. M. 1998 The biochemical basis of an all-or-none cell fate switch in *Xenopus* oocytes. *Science* **280**, 895–898. (doi:10.1126/science.280.5365.895)

Fournier, F. *et al.* 2008 Optical fingerprinting of peptides using two-dimensional infrared spectroscopy: proof of principle. *Anal. Biochem.* **374**, 358–365. (doi:10.1016/j.ab.2007.11.009)

Han, D. K., Eng, J., Zhou, H. L. & Aebersold, R. 2001 Quantitative profiling of differentiation-induced microsomal proteins using isotope-coded affinity tags and mass spectrometry. *Nat. Biotechnol.* **19**, 946–951. (doi:10.1038/nbt1001-946)

Hochmuth, F. M., Shao, J. Y., Dai, J. & Sheetz, M. P. 1996 Deformation and flow of membrane into tethers extracted from neuronal growth cones. *Biophys. J.* **70**, 358–369.

Huang, T. Y., Chu, T. F., Chen, H. I. & Jen, C. Y. J. 2000 Heterogeneity of $[Ca^{2+}]_i$ signaling in intact rat aortic endothelium. *FASEB J.* **14**, 797–804.

Huang, B., Wu, H. K., Bhaya, D., Grossman, A., Granier, S., Kobilka, B. K. & Zare, R. N. 2007 Counting low-copy number proteins in a single cell. *Science* **315**, 81–84. (doi:10.1126/science.1133992)

Hwang, W. C. & Waugh, R. E. 1997 Energy of dissociation of lipid bilayer from the membrane skeleton of red blood cells. *Biophys. J.* **72**, 2669–2678.

Jonsson, J. A. & Mathiasson, L. 2000 Membrane extraction techniques in bioanalysis. *Chromatographia* **52**, S8–S11. (doi:10.1007/BF02493110)

Leikin, S., Kozlov, M. M., Fuller, N. L. & Rand, R. P. 1996 Measured effects of diacylglycerol on structural and elastic properties of phospholipid membranes. *Biophys. J.* **71**, 2623–2632.

Li, Z., Anvari, B., Takashima, M., Brecht, P., Torres, J. H. & Brownell, W. E. 2002 Membrane tether formation from outer hair cells with optical tweezers. *Biophys. J.* **82**, 1386–1395.

Liu, Y., Cheng, D. K., Sonek, G. J., Berns, M. W., Chapman, C. F. & Tromberg, B. J. 1995 Evidence for localized cell heating induced by infrared optical tweezers. *Biophys. J.* **68**, 2137–2144.

Marcus, J. S., Anderson, W. F. & Quake, S. R. 2006 Parallel picoliter RT-PCR assays using microfluidics. *Anal. Chem.* **78**, 956–958. (doi:10.1021/ac0513865)

Neuman, K. C., Chadd, E. H., Liou, G. F., Bergman, K. & Block, S. M. 1999 Characterization of photodamage to *Escherichia coli* in optical traps. *Biophys. J.* **77**, 2856–2863.

Ocvirk, G., Salimi-Moosavi, H., Szarka, R. J., Arriaga, E. A., Andersson, P. E., Smith, R., Dovichi, N. J. & Harrison, D. J. 2004 Beta-galactosidase assays of single-cell lysates on a microchip: a complementary method for enzymatic analysis of single cells. *Proc. IEEE* **92**, 115–125. (doi:10.1109/JPROC.2003.820551)

Peirce, M. J., Wait, R., Begum, S., Saklatvala, J. & Cope, A. P. 2004 Expression profiling of lymphocyte plasma membrane proteins. *Mol. Cell Proteomics* **3**, 56–65. (doi:10.1074/mcp.M300064-MCP200)

Quinto-Su, P. A., Lai, H. H., Yoon, H. H., Sims, C. E., Allbritton, N. L. & Venugopalan, V. 2008 Examination of laser microbeam cell lysis in a PDMS microfluidic channel using time-resolved imaging. *Lab Chip* **8**, 408–414. (doi:10.1039/b715708h)

Rau, K. R., Quinto-Su, P. A., Hellman, A. N. & Venugopalan, V. 2006 Pulsed laser microbeam-induced cell lysis: time-resolved imaging and analysis of hydrodynamic effects. *Biophys. J.* **91**, 317–329. (doi:10.1529/biophysj.105.079921)

Raucher, D. & Sheetz, M. P. 1999 Characteristics of a membrane reservoir buffering membrane tension. *Biophys. J.* **77**, 1992–2002.

Roman, G. T., Chen, Y. L., Viberg, P., Culbertson, A. H. & Culbertson, C. T. 2007 Single-cell manipulation and analysis using microfluidic devices. *Anal. Bioanal. Chem.* **387**, 9–12. (doi:10.1007/s00216-006-0670-4)

Sakmann, B. & Neher, E. 1984 Patch clamp techniques for studying ionic channels in excitable membranes. *Annu. Rev. Physiol.* **46**, 455–472. (doi:10.1146/annurev.ph.46.030184.002323)

Schilling, E. A., Kamholz, A. E. & Yager, P. 2002 Cell lysis and protein extraction in a microfluidic device with detection by a fluorogenic enzyme assay. *Anal. Chem.* **74**, 1798–1804. (doi:10.1021/ac015640e)

Seddon, J. M. 1990 Structure of the inverted hexagonal (HII) phase, and non-lamellar phase-transitions of lipids. *Biochim. Biophys. Acta* **1031**, 1–69.

Sims, C. E. & Allbritton, N. L. 2007 Analysis of single mammalian cells on-chip. *Lab Chip* **7**, 423–440. (doi:10.1039/b615235j)

Szule, J. A., Fuller, N. L. & Rand, R. P. 2002 The effects of acyl chain length and saturation of diacylglycerols and phosphatidylcholines on membrane monolayer curvature. *Biophys. J.* **83**, 977–984.

Takayama, S., Ostuni, E., LeDuc, P., Naruse, K., Ingber, D. E. & Whitesides, G. M. 2003 Selective chemical treatment of cellular microdomains using multiple laminar streams. *Chem. Biol.* **10**, 123–130. (doi:10.1016/S1074-5521(03)00019-X)

Teruel, M. N. & Meyer, T. 2002 Parallel single-cell monitoring of receptor-triggered membrane translocation

of a calcium-sensing protein module. *Science* **295**, 1910–1912. (doi:10.1126/science.1065028)

Ward, A. D., Berry, M. G., Mellor, C. D. & Bain, C. D. 2006 Optical sculpture: controlled deformation of emulsion droplets with ultralow interfacial tensions using optical tweezers. *Chem. Commun.* 4515–4517. (doi:10.1039/b610060k)

Washburn, M. P., Wolters, D. & Yates, J. R. 2001 Large-scale analysis of the yeast proteome by multidimensional protein identification technology. *Nat. Biotechnol.* **19**, 242–247. (doi:10.1038/85686)

Waugh, R. E. & Bauserman, R. G. 1995 Physical measurements of bilayer-skeletal separation forces. *Ann. Biomed. Eng.* **23**, 308–321. (doi:10.1007/BF02584431)

Zhang, H. & Jin, W. R. 2006 Single-cell analysis by intracellular immuno-reaction and capillary electrophoresis with laser-induced fluorescence detection. *J. Chromatogr. A* **1104**, 346–351. (doi:10.1016/j.chroma.2005.11.083)

Zimmerberg, J. & Kozlov, M. M. 2006 How proteins produce cellular membrane curvature. *Nat. Rev. Mol. Cell Biol.* **7**, 9–19. (doi:10.1038/nrm1784)